

UNCLASSIFIED

AD NUMBER
ADB258643
NEW LIMITATION CHANGE
TO Approved for public release, distribution unlimited
FROM Distribution authorized to U.S. Gov't. agencies only; Proprietary Info.; Jul 99. Other requests shall be referred to U.S. Army Medical Research and Materiel Command, 504 Scott St., Fort Detrick, MD 21702-5012.
AUTHORITY
USAMRMC ltr, 28 May 2002

THIS PAGE IS UNCLASSIFIED

AD_____

GRANT NUMBER DAMD17-98-1-8232

TITLE: Development of Strategies to Manipulate ErbB Receptor
Heterodimerization from a Quantitative Analysis of
Receptor/Ligand Relationships

PRINCIPAL INVESTIGATOR: Mark A. Lemmon, Ph.D.

CONTRACTING ORGANIZATION: University of Pennsylvania
Philadelphia, Pennsylvania 19104-3246

REPORT DATE: July 1999

TYPE OF REPORT: Annual

PREPARED FOR: Commanding General
U.S. Army Medical Research and Materiel Command
Fort Detrick, Maryland 21702-5012

DISTRIBUTION STATEMENT: Distribution authorized to U.S. Government
agencies only (proprietary information, Jul 99). Other requests
for this document shall be referred to U.S. Army Medical Research
and Materiel Command, 504 Scott Street, Fort Detrick, Maryland
21702-5012.

The views, opinions and/or findings contained in this report are
those of the author(s) and should not be construed as an official
Department of the Army position, policy or decision unless so
designated by other documentation.

DTIC QUALITY INSPECTED 4

20001017 038

NOTICE

USING GOVERNMENT DRAWINGS, SPECIFICATIONS, OR OTHER DATA INCLUDED IN THIS DOCUMENT FOR ANY PURPOSE OTHER THAN GOVERNMENT PROCUREMENT DOES NOT IN ANY WAY OBLIGATE THE U.S. GOVERNMENT. THE FACT THAT THE GOVERNMENT FORMULATED OR SUPPLIED THE DRAWINGS, SPECIFICATIONS, OR OTHER DATA DOES NOT LICENSE THE HOLDER OR ANY OTHER PERSON OR CORPORATION; OR CONVEY ANY RIGHTS OR PERMISSION TO MANUFACTURE, USE, OR SELL ANY PATENTED INVENTION THAT MAY RELATE TO THEM.

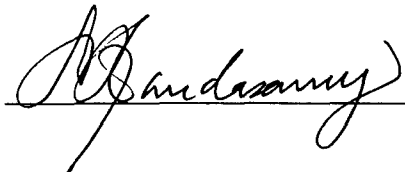
LIMITED RIGHTS LEGEND

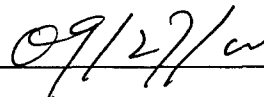
Award Number: DAMD17-98-1-8232

Organization: University of Pennsylvania

Those portions of the technical data contained in this report marked as limited rights data shall not, without the written permission of the above contractor, be (a) released or disclosed outside the government, (b) used by the Government for manufacture or, in the case of computer software documentation, for preparing the same or similar computer software, or (c) used by a party other than the Government, except that the Government may release or disclose technical data to persons outside the Government, or permit the use of technical data by such persons, if (i) such release, disclosure, or use is necessary for emergency repair or overhaul or (ii) is a release or disclosure of technical data (other than detailed manufacturing or process data) to, or use of such data by, a foreign government that is in the interest of the Government and is required for evaluational or informational purposes, provided in either case that such release, disclosure or use is made subject to a prohibition that the person to whom the data is released or disclosed may not further use, release or disclose such data, and the contractor or subcontractor or subcontractor asserting the restriction is notified of such release, disclosure or use. This legend, together with the indications of the portions of this data which are subject to such limitations, shall be included on any reproduction hereof which includes any part of the portions subject to such limitations.

THIS TECHNICAL REPORT HAS BEEN REVIEWED AND IS APPROVED FOR PUBLICATION.





FOREWORD

Opinions, interpretations, conclusions and recommendations are those of the author and are not necessarily endorsed by the U.S. Army.

Where copyrighted material is quoted, permission has been obtained to use such material.

Where material from documents designated for limited distribution is quoted, permission has been obtained to use the material.

Citations of commercial organizations and trade names in this report do not constitute an official Department of Army endorsement or approval of the products or services of these organizations.

NA In conducting research using animals, the investigator(s) adhered to the "Guide for the Care and Use of Laboratory Animals," prepared by the Committee on Care and use of Laboratory Animals of the Institute of Laboratory Resources, National Research Council (NIH Publication No. 86-23, Revised 1985).

NA For the protection of human subjects, the investigator(s) adhered to policies of applicable Federal Law 45 CFR 46.

NA In conducting research utilizing recombinant DNA technology, the investigator(s) adhered to current guidelines promulgated by the National Institutes of Health.

NA In the conduct of research utilizing recombinant DNA, the investigator(s) adhered to the NIH Guidelines for Research Involving Recombinant DNA Molecules.

NA In the conduct of research involving hazardous organisms, the investigator(s) adhered to the CDC-NIH Guide for Biosafety in Microbiological and Biomedical Laboratories.

For the protection of human subjects, the investigator(s) adhered to policies of applicable Federal Law 45 CFR 46.
MARK A. VERNON 7/29/99
PI - Signature Date

In conducting research utilizing recombinant DNA technology, the investigator(s) adhered to current guidelines promulgated by the National Institutes of Health. In the conduct of research utilizing recombinant DNA, the investigator(s) adhered to the NIH Guidelines for Research Involving Recombinant DNA Molecules.

TABLE OF CONTENTS

1.	FRONT COVER	1
2.	REPORT DOCUMENTATION PAGE	2
3.	FOREWORD	3
4.	TABLE OF CONTENTS	4
5.	INTRODUCTION	5
6.	BODY	6-24
7.	KEY RESEARCH ACCOMPLISHMENTS	25
8.	REPORTABLE OUTCOMES	26
9.	CONCLUSIONS	27
10.	REFERENCES	28
11.	APPENDICES	NONE

INTRODUCTION

Cellular responses to many extracellular factors that control cell growth and differentiation are mediated by cell-surface receptors with tyrosine kinase activity. The mechanism of transmembrane signaling by receptor tyrosine kinases involves an initial ligand-induced receptor dimerization event that leads to activation of the intracellular tyrosine kinase domain. For a given class of receptor tyrosine kinases, ligand-induced dimerization can involve two receptors that are the same (homodimerization) or different (heterodimerization). It is now appreciated that heterodimerization provides a mechanism for increasing the diversity of signaling through a given family of receptors. In our studies we focus on the four known receptors in the epidermal growth factor (EGF) receptor family - known as erbB1 to erbB4. The erbB receptors have been implicated in a number of human cancers. In particular, erbB2 (also known as Neu, or HER-2) is strongly implicated in breast cancer. Aberrant overexpression of a single member of this family can disrupt normal signaling, in some cases leading to uncontrolled cell proliferation. There are at least 12 different ligands that signal through the erbB family of receptor tyrosine kinases, including EGF, TGF α , and the neuregulins. The ligands differ in their receptor-binding characteristics, and appear to induce formation of distinct combinations of erbB receptor homo- and heterodimers. Their specific biological activities are thought to arise from these differences. We are interested in understanding how the multiple different ligands induce formation of particular receptor dimers. For the EGF receptor (erbB1), we previously showed that the extracellular domain is sufficient for ligand-induced dimerization, and that two EGF molecules are required to form the dimer. Through biophysical analyses of the other erbB receptor extracellular domains, produced in a baculovirus expression system, we have compared ligand-induced receptor homo- and heterodimerization by EGF and neuregulin-1 β (NRG1- β), the results of which are described in this report. Our current findings indicate that hetero-oligomerization or transmodulation of erbB receptors differs mechanistically from the accepted ligand-induced homodimerization model established for these and other receptors. Furthermore, while ligand-induced heterodimerization may be relevant for erbB2/erbB3/erbB4, it appears not to be important for the EGF receptor (erbB1). Our next goal is to incorporate the results of these studies of dimerization *in vitro* into an *in vivo* picture of signaling by this class of receptors. By developing this understanding, we hope that approaches will be suggested for specifically modulating erbB receptor signaling when it is disrupted in human cancers.

BODY OF PROGRESS REPORT

Progress for each task is detailed following description of the task

Task 1.

To determine quantitatively the hierarchy of erbB receptor homo- and heterodimers induced by each ligand in the EGF and NRG family

- *generate s-erbB proteins and erbB ligand in insect cells and yeast/bacteria, and perform preliminary qualitative studies of ligand-induced homo- and heterodimerization (months -18 to 0)*

We succeeded in producing milligram quantities of the four erbB receptor extracellular domains before funding of the award. Each of the four erbB receptor extracellular domains (s-erbB1, s-erbB2, s-erbB3, and s-erbB4) was secreted from Sf9 cells infected with recombinant baculovirus. Each s-erbB protein included the entire extracellular domain of the relevant receptor, followed by a hexahistidine tag to expedite purification from conditioned insect-cell medium. The most C-terminal native amino acid of each protein was K642 (s-erbB1); P647 (s-erbB2); K639 (s-erbB3); and R649 (s-erbB4); where residue numbers include the signal peptide.

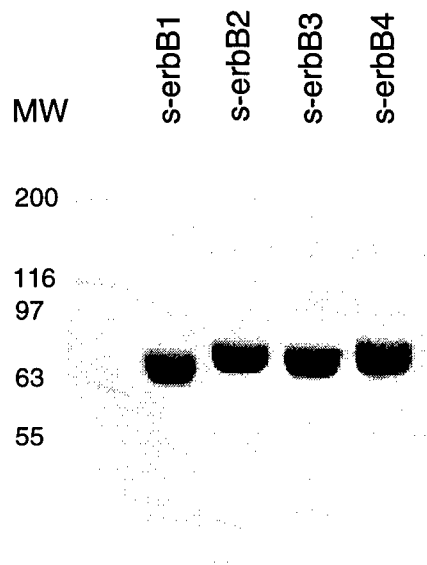


Figure 1

SDS-PAGE of the purified s-erbB proteins used for biophysical analyses of ligand-induced homo- and hetero-dimerization described in this progress report.

Using a Ni-NTA agarose column, followed by gel filtration and a single round of ion exchange (see Experimental Procedures), s-erbB proteins could be prepared from Sf9-cell conditioned, serum-free, medium with yields of 1.5 mg/liter (s-erbB1), 0.3 mg/liter (s-erbB2), 1 mg/liter (s-erbB3), and 0.8 mg/liter (s-erbB4). Significantly higher total yields could be achieved

Contains unpublished data

using High Five cells from *T. ni*, but the purified protein from these cells was more heterogeneous, and in some cases showed a tendency to aggregate. As a consequence, only protein secreted by Sf9 cells was employed in the studies described here. Figure 1 shows a Coomassie-stained SDS-PAGE gel of the purified s-erbB proteins, which we estimate to be greater than 92-95% pure in all cases.

We have focused most of our studies to date on the central ligands of the erbB ligand family: epidermal growth factor (EGF) and neuregulin-1 β 1 (NRG1- β 1). A number of experiments have also been performed with heparin-binding EGF-like growth factor (HB-EGF) and transforming growth factor- α (TGF- α). In all cases, commercially available ligands (from Interger or R & D Systems) have been employed. Our own efforts to express large quantities of erbB ligands in *Pichia pastoris* and *E. coli* yielded good quantities of EGF, which we have used for some experiments. However, NRG's, betacellulin, and TGF- α produced in these systems, while bio-active, were insufficiently homogeneous for use in our biophysical studies. Efforts are now underway to produce some of the key ligands not yet studied (notably betacellulin) in an insect cell system.

- *perform binding assays for each ligand to each possible combination of s-erbB proteins using calorimetric and SPR approaches (months 1 to 18)*

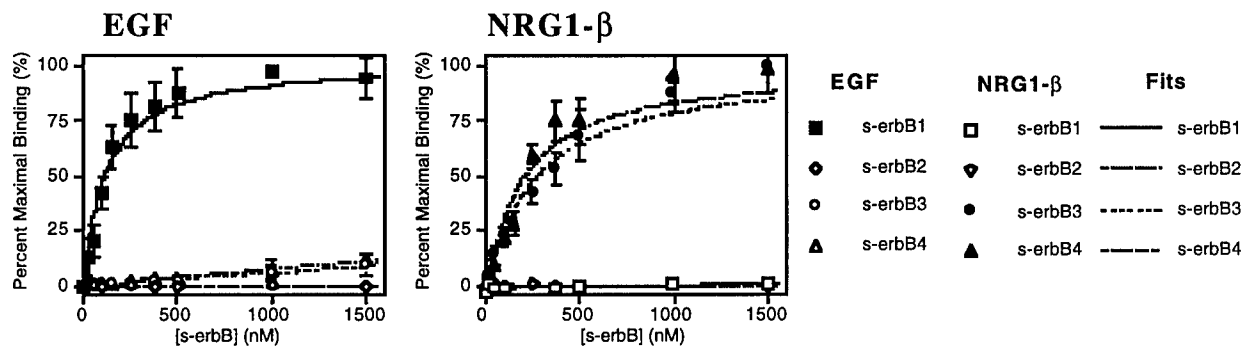
We have been able to use surface plasmon resonance (Biacore) to confirm that the s-erbB proteins secreted from Sf9 cells bind to the relevant growth factor ligands. Biacore CM-5 sensor chips were derivatized with the EGF-like domains of EGF or NRG1- β 1, or with no ligand, and solutions of the four purified s-erbB proteins were passed over the resulting surfaces. The results of these Biacore studies are summarized in Figure 2 and Table I. As anticipated, s-erbB1 bound significantly to the EGF-derivatized surface, but not to surfaces carrying NRG1- β 1 or no ligand. By contrast, s-erbB2 did not bind to any of the surfaces, and significant binding of s-erbB3 and s-erbB4 was seen only with surfaces bearing NRG1- β 1. Estimated K_D values for NRG1- β 1 binding by s-erbB3 and s-erbB4 were 249 nM and 179 nM respectively, and the estimated K_D for EGF binding by s-erbB1 was 118 nM (Table I). These K_D values all lie well within the range reported (100 to 500 nM) for EGF binding by monomeric s-erbB1 produced in mammalian cells (Greenfield *et al.*, 1989; Günther *et al.*, 1990; Hurwitz *et al.*, 1991; Lax *et al.*, 1991a; Zhou *et al.*, 1993; Brown *et al.*, 1994; Lemmon *et al.*, 1997). A K_D value of 17-35 nM was previously reported for binding of full-length NRG1- β 2 to monomeric s-erbB3 from analytical ultracentrifugation studies (Horan *et al.*, 1995). The 10-fold higher affinity seen by Horan *et al.*, may result from their use of full-length NRG1- β 2 rather than the EGF-like domain alone. However, the EGF-like domain is known to be sufficient for all known biological activities of

NRG1 (Holmes *et al.*, 1992). When binding of growth factors to predimerized IgG fusion proteins of erbB receptor extracellular domains is measured, the apparent affinities are approximately 30-fold higher (Jones *et al.*, 1998, 1999; Ballinger *et al.*, 1998; Fitzpatrick *et al.*, 1998). The relative binding affinities listed in Table I agree very well with the relative K_D or IC_{50} values reported from studies of IgG fusion proteins for EGF binding to s-erbB1 compared with binding of NRG1- β to erbB3 and erbB4.

Table I**Ligand binding by the s-erbB proteins**

Ligand	K_D for s-erbB1 (nM)	K_D for s-erbB2 (nM)	K_D for s-erbB3 (nM)	K_D for s-erbB4 (nM)
EGF	118 ± 41	none	$> 10^4$	$> 10^4$
NRG- β 1	$> 10^5$	none	249 ± 80	179 ± 10

Summary of K_D measurements made for the four s-erbB proteins to immobilized EGF and NRG1- β 1. K_D values listed explicitly represent means of at least four independent determinations, and are quoted alongside their standard deviations.

**Figure 2**

Binding of s-erbB1, s-erbB2, s-erbB3, and s-erbB4 to EGF (left) and NRG1- β 1 (right), immobilized on a BIAcore chip. Best-fits to the data, assuming a simple association model, are shown. Errors are standard deviations from the mean of at least 4 independent determinations at each point. K_D values represented by the best fits are list in Table I.

We have not been able to detect any significant difference in binding affinities when passing over mixtures of s-erbB proteins. In particular, a mixture of s-erbB2 and s-erbB4 gave results for NRG1- β binding that were not clearly distinguishable from those determined with s-erbB4 alone (Figure 2), despite the fact that NRG1- β induces s-erbB2/s-erbB4 heterodimer formation. Titration calorimetry was employed to study EGF binding to s-erbB1, and results

identical to those obtained previously (Lemmon et al., 1997) were obtained. Given the relative difficulty of interpreting calorimetric results for dimerization-coupled binding events, and the large quantities of material required for these studies, we have settled upon BIAcore measurements as a more expeditious approach.

- *using classical multi-angle laser light scattering methods, measure the ability of each erbB ligand to induce homodimerization of each s-erbB protein, by varying both ligand and receptor concentration (months 1 to 4)*

As shown in Figure 3, multi-angle laser light-scattering (MALLS) was measured for a series of samples containing s-erbB protein at 4 μ M, to which had been added increasing concentrations of EGF or NRG1- β 1. The weight-averaged molecular mass (M_w) for each sample, relative to that measured in the absence of ligand, was determined by extrapolation of a Debye plot to zero angle and was expressed as a fold-increase in M_w (see Experimental Procedures). As shown in Figure 3, addition of one molar equivalent of EGF to s-erbB1 resulted in a doubling of M_w , as we have observed previously in X-ray scattering studies (Lemmon *et al.*, 1997). No further increase in M_w was seen when larger excesses of EGF were added, consistent with our previous finding that EGF induces formation of a 2:2 s-erbB1:EGF dimer, but no higher order oligomers (Lemmon *et al.*, 1997).

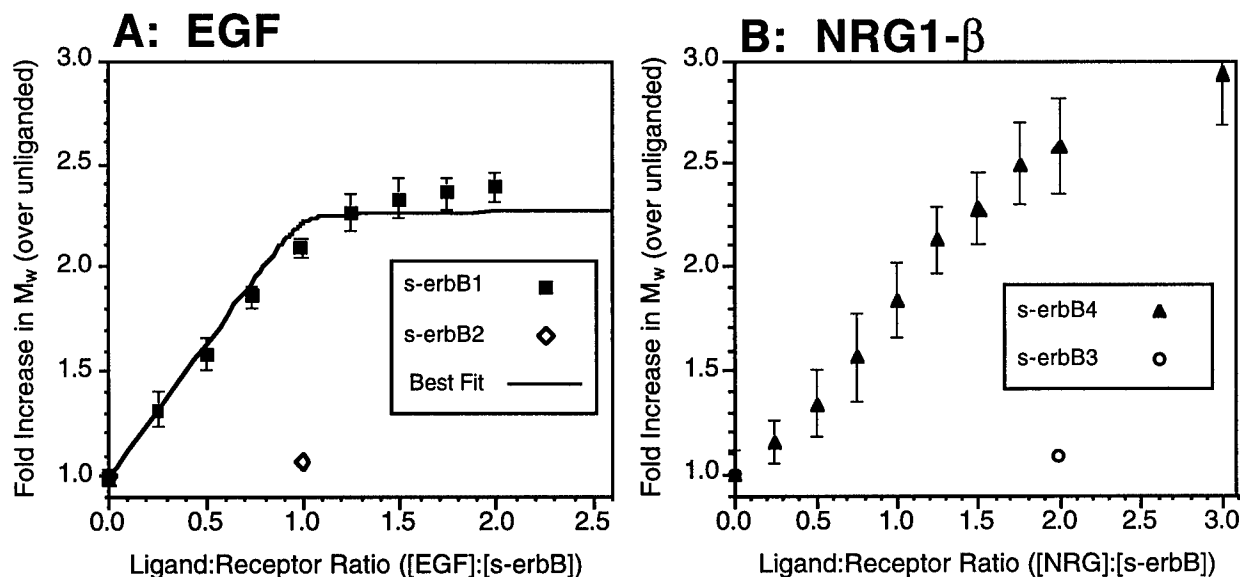


Figure 3

MALLS studies of EGF-induced homo-dimerization of s-erbB1 and s-erbB2 (A) as well as of NRG1- β 1 induced homodimerization of s-erbB3 and s-erbB4 (B) (see text).

Figure 3A shows a best fit to the EGF-induced s-erbB1 dimerization data using a model in which a 1:1 EGF:s-erbB1 complex forms with $K_D = 118$ nM, and this 1:1 complex dimerizes with K_D less than 100 nM to form the 2:2 EGF:s-erbB1 dimer. This data fitting indicates that our insect cell-derived s-erbB1 dimerizes 20 to 50-fold more strongly than the CHO cell-derived protein studied by Lemmon *et al.*

Analysis of s-erbB4 by MALLS also demonstrated clear dimerization upon addition of NRG1- β 1. In this case, the maximum M_w is not reached until almost two equivalents of NRG1- β 1 have been added to the s-erbB4. Furthermore, in some experiments the final M_w was a little higher than expected for a 2:2 s-erbB4:NRG1- β 1 complex. These MALLS experiments, together with our analytical ultracentrifugation studies, argue against the possibility that NRG1- β 1 induces formation of s-erbB4 oligomers with order greater than two. However, the data are consistent with a model similar to that described for EGF-induced s-erbB1 dimerization if it is assumed that 20 to 30% of the NRG1- β 1 preparation is present as small aggregates and/or is inactive. Given this caveat, we have not attempted to fit the NRG1- β 1/s-erbB4 data explicitly, although it is clear that NRG1- β 1 induces strong s-erbB4 dimerization.

As also shown in Figure 3, addition of excess EGF to s-erbB2 does not induce its dimerization (Fig 3A), and addition of excess NRG1- β 1 to s-erbB3 does not significantly increase M_w of that protein (Fig 3B). Thus, these data argue that EGF induces homodimerization of only s-erbB1, and NRG1- β 1 induces homodimerization of only s-erbB4. Homodimers of neither s-erbB2 nor s-erbB3 can be induced by these ligands or any other tested.

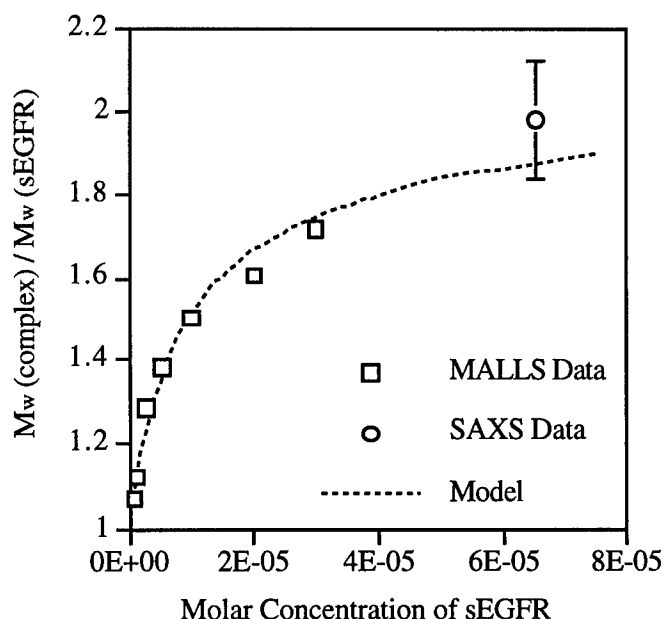


Figure 4
Measurement of \bar{M}_w for a 1:1 EGF/s-erbB1 mixture at a series of different molar concentrations in 50 mM Hepes, pH 7.5, 100 mM NaCl at 25°C. Data up to 30 μ M were obtained from MALLS measurements, while the data point at 65 μ M is an average of the relative \bar{M}_w measured for a 1:1 mixture in small-angle X-ray scattering (SAXS) experiments. The solid line represents predicted data from the model presented by Lemmon *et al.*, (1997), with K_f increased to 8 μ M and K_b reduced to 25 μ M as described in the text. The error on the Debye plot fit for each MALLS data point does not extend beyond the symbol size.

To determine K_D values for ligand-induced s-erbB1 and s-erbB4 homodimerization, experiments were performed in which the concentration of a 1:1 receptor:ligand complex was varied, as shown in Figure 4. For the CHO cell-derived s-erbB1 that we employed prior to the beginning of these studies, this approach was useful, and gave a dimerization K_D of approximately 3 μ M to 8 μ M, depending on the batch of protein employed. The protein that we now produce from insect cells dimerizes much more strongly, such that we have not been able to detect dissociation of the dimer in complex dilution experiments of this sort. Data fitting suggests that K_D for s-erbB1 or s-erbB4 homodimerization, when occupied by EGF or NRG1- β 1 respectively, is in the 30 nM range. The precision of this value will be improved through analytical ultracentrifugation experiments to be performed over the coming months.

- *using the results from the homodimerization assay, assess using light-scattering the ability of each erbB ligand to induce each of the 6 possible s-erbB heterodimers. By repeating experiments using different concentrations of receptors and ligands (and different ratios of the two s-erbB proteins), determine binding constants for dimerization and ligand binding (months 1 to 12)*

The most likely relevant erbB receptor heterodimer or oligomer in breast cancer, and the one that was first reported to occur, is the erbB1/erbB2, or EGFR/Neu hetero-oligomer (King *et al.*, 1988; Stern *et al.*, 1988; Wada *et al.*, 1990). Having established (as described above) that EGF induces efficient s-erbB1 homodimerization, and that NRG1- β 1 induces efficient s-erbB4 homodimerization, we next tested the ability of these s-erbB proteins to heterodimerize upon growth factor binding. As outlined in the introduction, there is a great deal of evidence for ligand-induced heterodimerization of erbB receptors. One of the first indications for heterodimerization (or transmodulation) came from the finding that erbB2, which does not bind EGF, can nonetheless be activated by EGF in cells that express both erbB1 and erbB2 (King *et al.*, 1988; Stern *et al.*, 1988; Wada *et al.*, 1990; Spivak-Kroizman *et al.*, 1992). ErbB2 is not activated by EGF in cells that do not express erbB1. Transmodulation of erbB2 by erbB1 has been shown to result from EGF-dependent association of erbB1 and erbB2 to form presumed heterodimers that show elevated tyrosine kinase activity, and are extensively autophosphorylated (Wada *et al.*, 1990; Spivak-Kroizman *et al.*, 1992). Supporting the suggestion that erbB1/erbB2 heterodimers might resemble active erbB1 homodimers, erbB2 with a cytoplasmic truncation was reported to act as a dominant-negative inhibitor of erbB1 signaling (Qian *et al.*, 1994) apparently in the same way as similar erbB1 truncation mutants inhibit EGF signaling (Kashles *et al.*, 1991).

Since EGF efficiently induces s-erbB1 homodimerization (see above), we reasoned from findings in the literature and current models for heterodimerization that EGF should also induce efficient heterodimerization of s-erbB1 and s-erbB2.

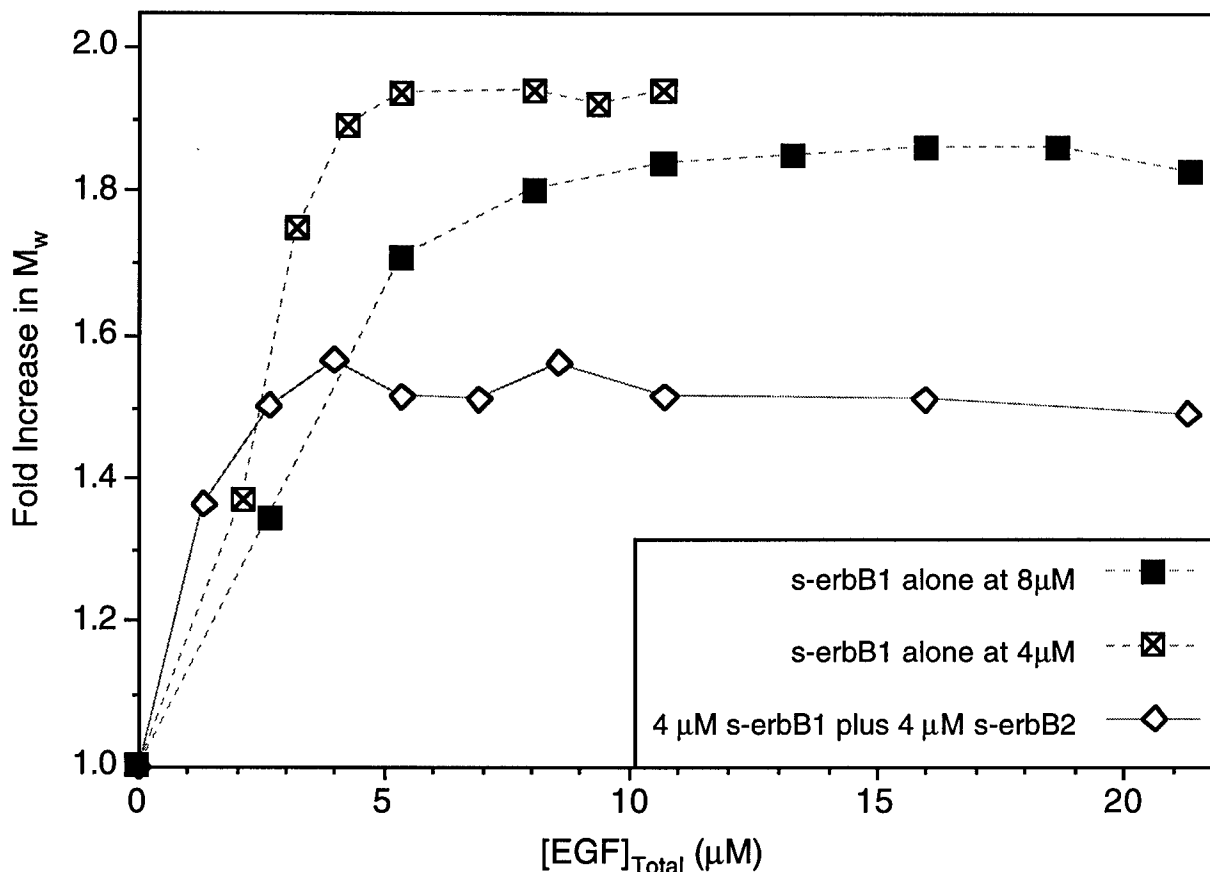


Figure 5

MALLS studies demonstrate that EGF induces complete homodimerization of s-erbB1, but does not induce formation of heterodimers between s-erbB2 and s-erbB1. The weight-averaged molecular mass (M_w) of the s-erbB1/s-erbB2 mixture increases such that after addition of one EGF molecule for each s-erbB1 molecule in the mixture, M_w reaches a maximum coincident with all s-erbB1 forming homodimers, and s-erbB2 remaining monomeric.

Figure 5 presents our MALLS studies, which show that EGF is not able to induce the expected extracellular domain heterodimerization. MALLS monitors the weight-averaged molecular mass (M_w) of the particles in solution. For a sample containing only 4 μM s-erbB1, M_w is doubled upon addition of greater than 4 μM EGF (Figure 5 crossed squares). Similarly, for a sample containing 8 μM s-erbB1, M_w is almost doubled when more than 8 μM EGF is added (Figure 5 filled squares). By contrast, for a sample containing 4 μM s-erbB1 plus 4 μM s-erbB2, M_w reaches a maximum value when EGF is added to a final concentration of 4 μM (Figure 5, open diamonds). The fold-increase in M_w in this case is only 1.5. This is the expected result if

EGF induces s-erbB1 homodimerization while s-erbB2 remains monomeric in the mixture. M_w is defined:

$$\overline{M}_w = \frac{\sum_i n_i M_i^2}{\sum_i n_i M_i} \quad \text{for } n \text{ moles of } i \text{ different species with molecular mass } M_i$$

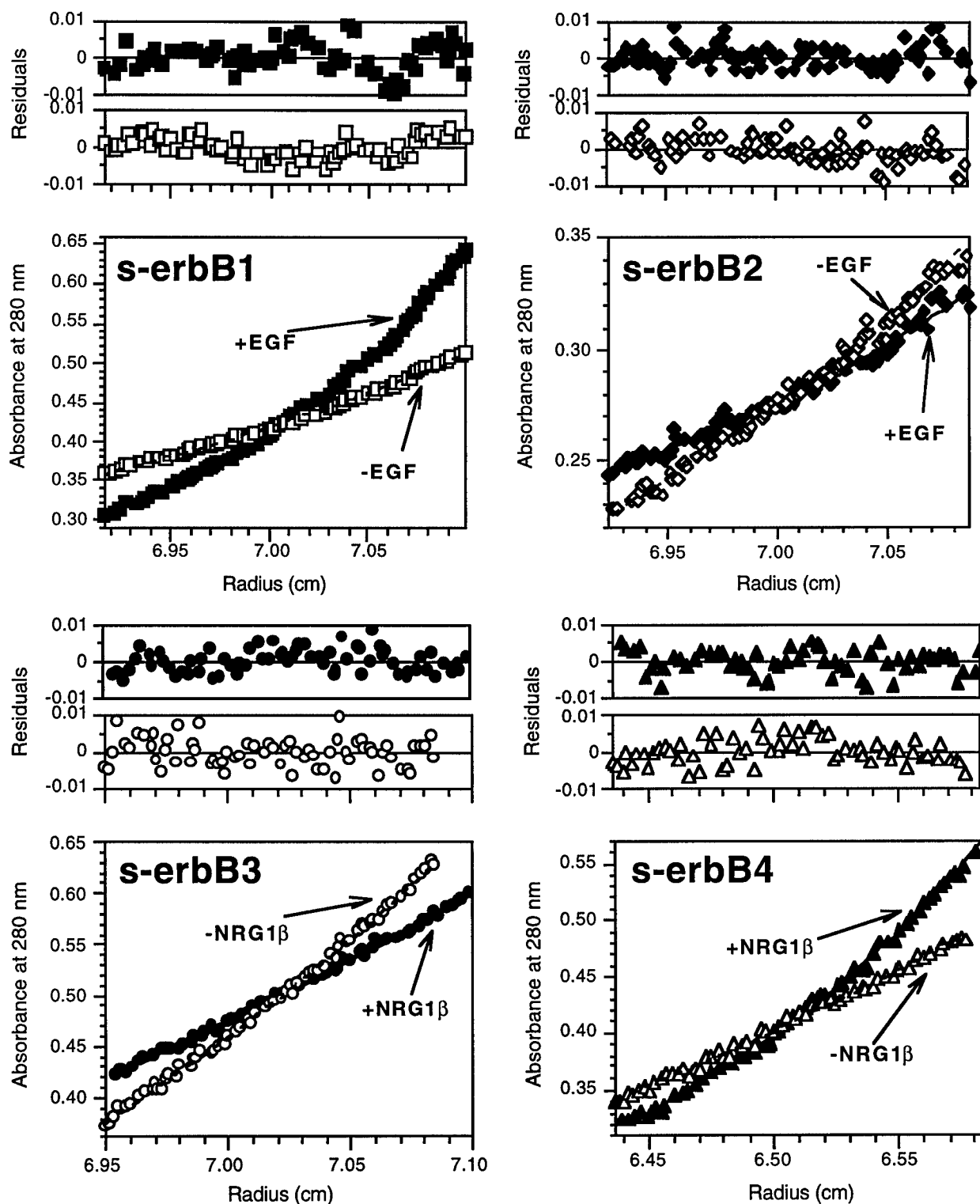
In a sample containing 4 μ M monomeric s-erbB2 (80 kDa) plus 2 μ M s-erbB1 dimers (160 kDa), M_w would be estimated as 120 kDa, or a 1.5-fold increase over the monomeric M_w of 80 kDa. Thus, the MALLS data provide no evidence for EGF-induced s-erbB1/s-erbB2 heterodimerization, and argue that s-erbB1 in the mixture homodimerizes with s-erbB2 as a monomeric “bystander”.

These results suggest that the ligand-induced erbB1/erbB2 hetero-oligomers observed by several groups must form through a mechanism distinct from that used by erbB1 for homodimerization upon EGF binding. In the homomeric case, the isolated extracellular domain can recapitulate the interaction. In the heteromeric case it cannot. However, one caveat to this finding is that we have no independent validation of the functional quality of our s-erbB2 preparations. Since erbB2 has no known ligand, we cannot validate the protein by virtue of its ability to bind ligand, as was done for s-erbB1, s-erbB3, and s-erbB4 (Figure 2). However, we do not believe that the s-erbB2 is non-functional, since it is able to form NRG1-induced heterodimers with both s-erbB3 and s-erbB4 (see below). Furthermore, MALLS studies of potential heterodimers formed between s-erbB1 and s-erbB3 or s-erbB4 (with EGF or NRG1- β 1) also gave clear negative results (not shown). Thus, in spite of its ability to form EGF-induced homodimers, s-erbB1 does not form heterodimers with other isolated erbB receptor extracellular domains.

MALLS studies have given indications of NRG1- β 1-induced heterodimer formation for s-erbB2/s-erbB4 and s-erbB2/s-erbB3. Datasets for these MALLS studies are currently being completed. Moreover, as detailed below, analytical ultracentrifugation studies illustrate the formation of these heterodimers.

- *confirm findings regarding ligand-induced s-erbB homo- and heterodimerization in vitro using analytical ultracentrifugation (month 1-18)*

Using sedimentation analytical ultracentrifugation and multi-angle laser-light scattering (MALLS), we have studied ligand-induced dimerization of each s-erbB protein. Figure 6 shows typical results from sedimentation equilibrium experiments (6,000 rpm) in which samples of each s-erbB protein were centrifuged both with and without the most relevant growth factor ligand.

**Figure 6**

Representative sedimentation equilibrium analytical ultracentrifugation data for analysis of s-erbB homodimerization induced by EGF or NRG1- β 1. In each case, open symbols represent the unliganded receptor, which is fit as an ideal single species (molecular mass range from 80 kDa for s-erbB1 to 97 kDa for s-erbB4). Filled symbols represent samples to which has been added a two-fold molar excess of the noted ligand. Fits to these data are with two ideal

Contains unpublished data

species - fixing the Mw of the ligand and floating the Mw of the complex. Fits return Mw of 198 kDa for s-erbB1 (dimer), 77.5 kDa for s-erbB2 (monomer), 85 kDa for s-erbB3 (monomer), and 197 kDa for s-erbB4 (dimer). As described in the text, this result is clear from inspection of the curves. All experiments shown were performed at 6,000 rpm (other speeds giving the same result). Residuals for the fits described are shown, and are both small and random, indicative of a good fit.

Inspection of the raw centrifugation data in Figure 6 shows that addition of a 2-fold molar excess of EGF to s-erbB1, or of a 2-fold excess of NRG1- β 1 to s-erbB4 (filled symbols) results in a radial distribution indicative of a species larger than the s-erbB protein monomer. Since the s-erbB proteins have molecular masses of around 85 kDa, and the added ligands have molecular masses of only 6.3 kDa (EGF) and 8.3 kDa (NRG1- β 1), this can only be explained if the s-erbB protein is induced to oligomerize upon addition of the growth factor. Data fitting assuming a single ideal species for the ligand-free receptor gives molecular masses of 80 kDa and 97 kDa for s-erbB1 and s-erbB4 respectively. The best fit to the ligand/receptor mixture is obtained with two ideal species representing excess ligand and the s-erbB dimer. The residuals for these fits (experimental value minus fit value), plotted above the data in Figure 6, are both small and random, indicative of good fits to the data.

By contrast with the case for s-erbB1 and s-erbB4, addition of excess ligand to s-erbB2 or s-erbB3 results in a radial distribution consistent with a single species that is smaller than monomeric s-erbB protein. This is the expected result if the s-erbB protein does not bind ligand, or does not oligomerize upon ligand binding, since the distribution is now contributed to by free ligand that is 10-fold smaller (6 to 8 kDa) than the s-erbB protein (approx. 85 kDa). While best fits to a single ideal species gave molecular masses of 80.8 kDa and 84 kDa for s-erbB2 and s-erbB3 (without ligand) respectively, best fits to the ligand/receptor mixtures were obtained with two ideal species representing excess ligand and the s-erbB monomer (77.5 and 85 kDa for s-erbB2 and s-erbB3 respectively). Again, residuals for these fits are plotted above the data in Figure 3, and are both small and reasonably random, suggesting reasonable fits.

These data confirm the MALLS finding that, while s-erbB1 and s-erbB4 dimerize upon binding to EGF and NRG1- β 1 respectively, s-erbB3 does not dimerize when it binds NRG1- β 1. The inability of EGF to induce s-erbB2 dimerization is consistent with the lack of significant binding (Figure 2). NRG1- β 1 also failed to bind s-erbB2 or to induce its dimerization (Figure 2 and 9). In other sedimentation equilibrium experiments (not shown) we found that s-erbB1 dimerization is also induced by TGF- α and HB-EGF (to which it binds), but not by NRG1- β 1 (to which it does not bind). Dimerization of s-erbB4 was seen with NRG1- β 1 (to which it binds), but not with HB-EGF, or EGF (to which it does not bind in our hands). Thus, all ligands tested that are capable of binding to s-erbB1 or s-erbB4 also induce their homodimerization. The failure of neuregulins to induce homodimerization of s-erbB3 represents the only example we have seen in

which binding is observed in the absence of associated homodimerization. Previous studies with full-length NRG1- β 1 (Horan *et al.*, 1995) also showed strong binding to s-erbB3 in the absence of induced dimerization.

Also using analytical ultracentrifugation, we have confirmed the inability of EGF to induce s-erbB1/s-erbB2 heterodimerization (Figure 7), and the failure of NRG1- β 1 to induce s-erbB1/s-erbB4 heterodimerization (Figure 8). Figure 7 shows plots of the natural logarithm of absorbance against $(r^2 - r_0^2)/2$, where r is the radial position in the sample, and r_0 the radial position of the meniscus for datasets collected at 6,000 rpm. For an ideal single species this plot is linear, with a gradient $(M\omega^2(1 - \bar{V}_2\rho)/RT)$ that is proportional to the molecular mass (M) of the ideal species. The lines obtained for s-erbB1 alone and s-erbB2 alone are approximately the same, and yield molecular masses of 80.5 and 78.9 kDa respectively. Addition of one equivalent of EGF to s-erbB1 results in near doubling of the gradient of this line, consistent with the ability of EGF to induce complete dimerization of s-erbB1. By contrast, addition of EGF to a 1:1 mixture of s-erbB1 and s-erbB2 increases the gradient of the line to only an intermediate extent (1.3-fold) and causes a greater deviation from linearity. This result is consistent with the interpretation of MALLS studies (Figure 5) that EGF induces homodimerization of s-erbB1 in the s-erbB1/s-erbB2 sample while the s-erbB2 remains monomeric.

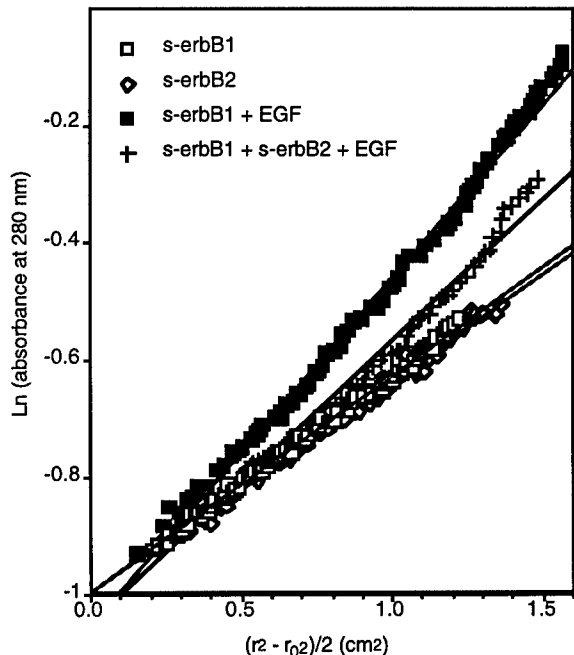


Figure 7

Plots of the natural logarithm of absorbance against the radius squared for analytical ultracentrifugation data. S-erbB1 and s-erbB2 alone yield straight lines in this plot, with gradients proportional to their molecular mass. Addition of EGF to s-erbB1 doubles the gradient showing that dimerization results. For an s-erbB1/s-erbB2 mixture, addition of a 2-fold excess of EGF yields an increase in the gradients of only about 1.3-fold. As in Fig 5, this is expected as the s-erbB1 homodimerizes while s-erbB2 remains monomeric.

These experiments, together with chemical crosslinking studies and co-immunoprecipitation studies (not shown), confirm the MALLS finding that EGF is not able to induce heterodimerization of the isolated extracellular domains of erbB1 and erbB2.

Heterodimerization of erbB1 and erbB4 upon treatment with EGF or NRG has been reported by several groups (*e.g.* Cohen *et al.*, 1996; Zhang *et al.*, 1996). Since we have been able to show that s-erbB1 and s-erbB4 both bind to their relevant ligands and homodimerize efficiently (Figures 3 and 6), we can be confident that both of these proteins are functionally active. We next used analytical ultracentrifugation to determine whether s-erbB1 and s-erbB4 can form heterodimers upon treatment with EGF or NRG1- β 1.

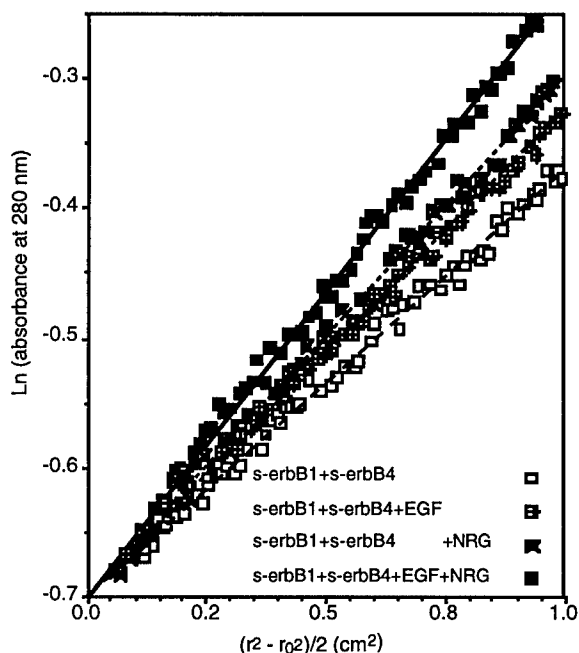


Figure 8

Analytical ultracentrifugation data, presented as $\ln(\text{Abs})$ against r^2 plots, for s-erbB1/s-erbB4 heterodimerization. The s-erbB1/s-erbB4 mixture without ligand gives a straight line with gradient that yields monomer molecular mass. Addition of one molar equivalent (to total receptor) of EGF alone, or of NRG alone results in an increase in molecular mass consistent with homodimerization of one species only. Addition of both EGF and NRG at the same level results in a substantial increase in the gradient, indicating that both species are homodimerizing independently (see text for explanation).

Figure 8 presents $\ln(\text{Abs})$ against $(r^2 - r_0^2)/2$ plots for a series of 1:1 s-erbB1/s-erbB4 mixtures. The total receptor concentration is the same in each case. With no added ligand, the gradient of the straight line (proportional to molecular mass when an ideal single species is considered) gives an average monomeric molecular mass of approximately 80 kDa when divided by the appropriate constants. Addition of EGF to a concentration twice that of total receptor (*i.e.* 2 EGF molecules per s-erbB1 plus 2 EGF molecules per s-erbB4) increases the gradient of the straight line by a factor of approximately 1.3, suggesting that some dimerization is induced. Addition of NRG1- β 1 to the same final concentration gives a similar result. Note that ligand is not limiting in either of these cases, suggesting that the limited increase in gradient results from homodimerization of only s-erbB1 when EGF is added, and only s-erbB4 when NRG1- β 1 is added. If this is true, then an identical sample containing the same total ligand concentration, but as a mixture of EGF and NRG1- β 1 should show substantially more dimerization, as both s-erbB1 and s-erbB4 will be capable of homodimerizing independently. The steepest line in Figure 8 shows this to be the case, providing evidence that, as with s-erbB1 and s-erbB2, hetero-

dimerization of s-erbB1 and s-erbB4 does not occur under these conditions - with either EGF or NRG1- β 1. In similar experiments we have shown that s-erbB1 also fails to form heterodimers with s-erbB3, regardless of whether EGF or NRG1- β 1 is added. Thus, we have failed to detect formation of any heterodimer that includes s-erbB1.

Heterodimerization between NRG-binding receptors and s-erbB2

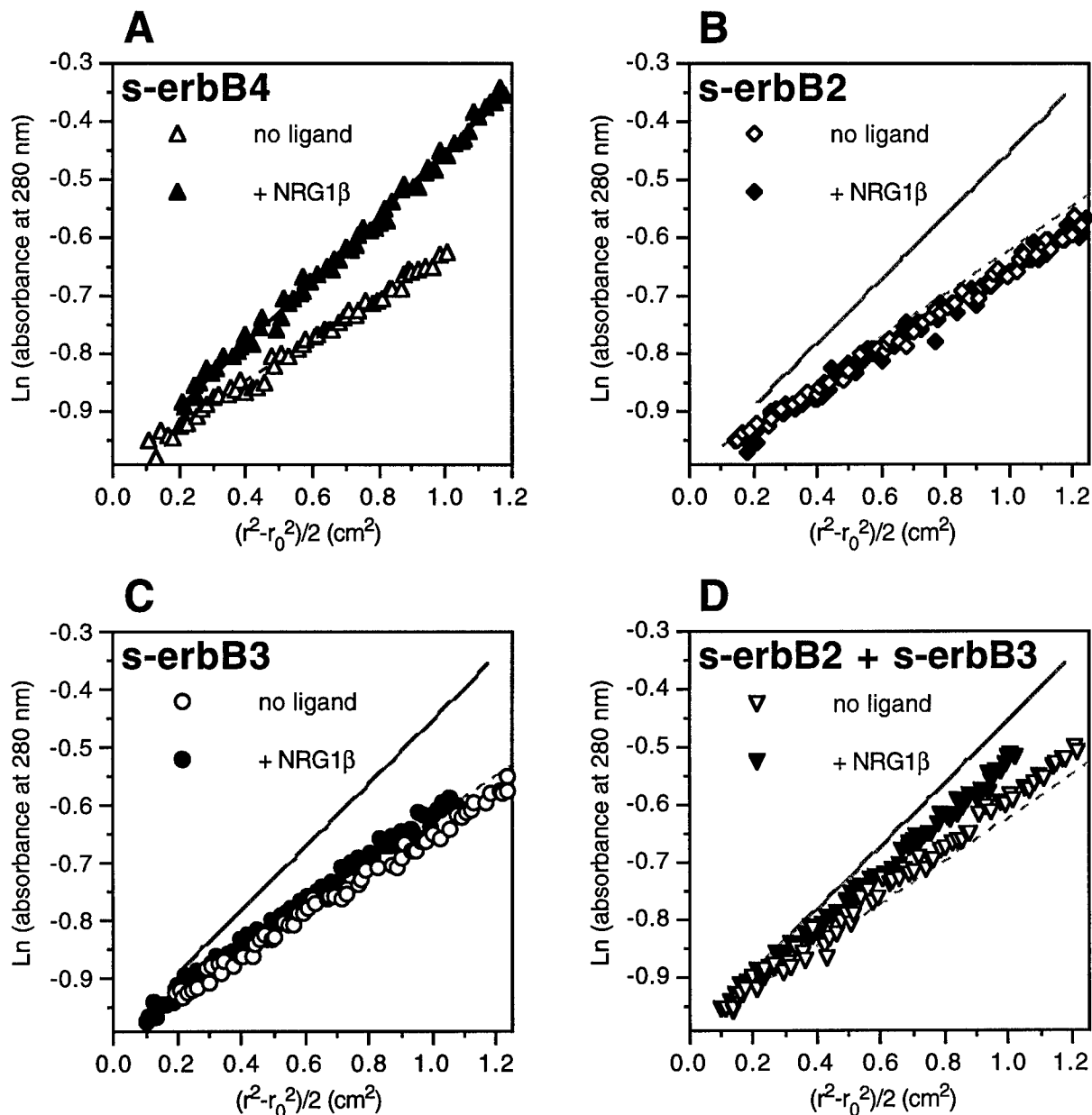
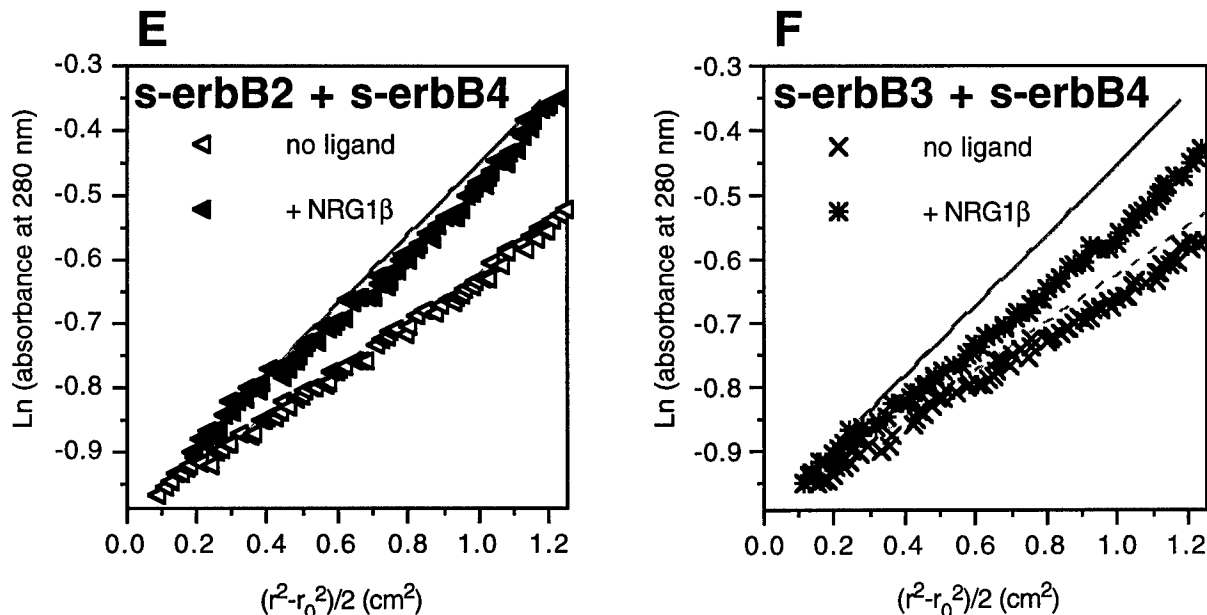


Figure 9

Analytical ultracentrifugation evidence for formation of s-erbB2/s-erbB3 and s-erbB2/s-erbB4 heterodimers. Panel A shows the increase in gradient of the $\ln(\text{Abs})$ against r^2 plot that results from NRG1- β 1-induced s-erbB4 homodimerization. These lines are superimposed in grey on all other panels. Panels B and C show that NRG1- β 1

Contains unpublished data

fails to induce homodimerization of s-erbB2 or s-erbB3, while panels D and E demonstrate that NRG1- β 1 can induce formation of s-erbB2/s-erbB3 and s-erbB2/s-erbB4 heterodimers. Panel F indicates that s-erbB3 and s-erbB4 do not heterodimerize efficiently upon NRG1- β 1 binding.



Using a similar approach to that used for investigating s-erbB1/s-erbB2 and s-erbB1/s-erbB4 heterodimerization, we next tested the ability of s-erbB3 and s-erbB4 to heterodimerize with one another and with s-erbB2. Recent studies by Sliwkowski's laboratory (Fitzpatrick *et al.*, 1998; Jones *et al.*, 1999) have shown that dimeric IgG fusion proteins containing s-erbB2 together with either s-erbB3 or s-erbB4 have an enhanced affinity for NRG compared with those containing just s-erbB3 or just s-erbB4. This finding has been interpreted to suggest that s-erbB2/s-erbB3 and s-erbB2/s-erbB4 heterodimers represent high-affinity NRG receptors. In Figure 9, ln(Abs) versus radius² plots are shown for each pairwise combination of s-erbB2, s-erbB3, and s-erbB4 with and without NRG1- β 1. In panel A, NRG-induced homodimerization of s-erbB4 is clearly seen by the approximately 1.6-fold increase in gradient upon addition of a 2-fold excess of NRG1- β 1. No such increase is seen upon addition of NRG1- β 1 to s-erbB2 (panel B) or s-erbB3 (panel C). In panel D it can be seen that NRG1- β 1 induces a small increase in the gradient of the ln(Abs) against r² line for an s-erbB2/s-erbB3 mixture. The increase is less dramatic than that seen for s-erbB4, and there may be some tendency for these two s-erbB proteins to interact with one another in the absence of ligand (the gradient is slightly greater than that for the ligand-free mixture than for any unliganded s-erbB protein). However, the NRG-induced shift in gradient shown here is reproducible, and suggests some weak ligand-induced heterodimerization of s-erbB2 and s-erbB3.

Comparing panel F with Figures 7 and 8, it can be seen that the s-erbB3/s-erbB4 mixture behaves, when NRG1- β 1 is added, in the same way as an s-erbB1/s-erbB4 mixture with NRG1- β 1 or either a s-erbB1/s-erbB2 or s-erbB1/s-erbB4 mixture when EGF is added. In other words, addition of NRG1- β 1 appears to induce s-erbB4 homodimerization while s-erbB3 remains monomeric. There is therefore no evidence for s-erbB3/s-erbB4 heterodimerization. However, panel E of Figure 9 appears almost identical to panel A, despite the fact that the mixture contains s-erbB2 that neither binds NRG1- β 1 nor is induced to dimerize by this ligand. The only explanation for this result is that NRG1- β 1 induces efficient heterodimerization of s-erbB2 and s-erbB4. This finding allays our fears that negative results with s-erbB1/s-erbB2 heterodimerization simply reflect a non-functional s-erbB2 preparation.

EXPERIMENTAL PROCEDURES

Generation of s-erbB Constructs

A fragment of human erbB1 cDNA directing expression of residues 1-642 (1-618 of the mature sequence) followed by a hexahistidine tag and stop codon was subcloned into pFastBac1 (Life Technologies Inc). The 1955-base pair fragment was generated by PCR, introducing a unique *Bgl* II site immediately before the initiation codon and a unique *Xba* I site that follows the introduced stop codon. The 1955-base pair *Bgl* II/*Xba* I digested PCR product was ligated into *Bam* HI/*Xba* I digested pFastBac I. To minimize the risk of PCR artifacts, a 1260-base pair *Eco* RI/*Apa* I fragment of this PCR-derived clone was swapped for the equivalent region from the original erbB1 cDNA.

A fragment of human erbB2 cDNA directing expression of residues 1-647 (1-628 of the mature sequence) was generated similarly. In this case a unique *Xba* I site was introduced before the initiation codon, and a unique *Hind* III site was introduced to follow the histidine tag and stop codon. The 1980-base pair *Xba* I/*Hind* III digested PCR product was ligated into *Xba* I/*Hind* III-digested pFastBac I. An 1880-base pair internal fragment of this PCR product, extending from an *Nco* I site at the initiation codon to a unique *Sph* I site, was then swapped for the equivalent fragment from the original erbB2 cDNA.

Fragments encoding human erbB3 residues 1-639 (1-620 of the mature protein) and human erbB4 residues 1-649 (1-624 of the mature protein), with a unique *Bam* HI site at one end and *Xba* I site at the other, were generated by PCR, and ligated into *Bam* HI/*Xba* I digested pFastBac I. The sequence of all PCR-derived fragments and their cloning boundaries were confirmed by standard manual or automated dideoxynucleotide sequencing methods.

Protein Production

Typically 5 - 10 liters of Sf9 cells were grown as a suspension culture in Sf900-II medium (Gibco/BRL) using a number of 1 liter spinner flasks. Each 1 liter flask contained less than 500 ml of medium to ensure adequate aeration. When a cell density of 2.5×10^6 cells/ml (viability >98%) was reached, freshly amplified high-titer virus stock was added to a multiplicity of infection (MOI) of approximately 5. Cultures were incubated for a further 96 hours. Clarified conditioned medium was then diafiltered against 3.5 volumes of 25 mM Tris-HCl, 150 mM NaCl, pH 8.0 (buffer A), using a Millipore Prep/Scale-TFF 30 kDa cartridge, and was concentrated to approximately 300 ml prior to loading onto a 5 ml Ni-NTA Superflow column (Qiagen). After extensive washing with buffer A, the column was washed sequentially with 2 column volumes of buffer A containing 30, 50, 75, 100 and 300 mM imidazole, pH 8.0. Typically the majority of the protein eluted in the 75 and 100 mM fractions. Fractions were concentrated in a Centriprep 30 (Amicon), and loaded onto a Pharmacia Superose 6 gel filtration column. The s-erbB proteins eluted as approximately 85 kDa species, and were greater than 95% pure at this stage of purification. For s-erbB1 and s-erbB4, appropriate gel-filtration fractions were pooled, diluted 1.5 fold with 50 mM MES pH 6.0, and were loaded on to an BioScale-S2 cation exchange column (BioRad), pre-equilibrated with 25 mM MES pH 6.0. Protein was eluted with a gradient in NaCl, s-erbB1 eluting at approximately 200 mM NaCl, and s-erbB4 at approximately 300 mM NaCl. Attempts to purify s-erbB2 and s-erbB3 by ion exchange led only to precipitation of the proteins at the low salt concentration required for binding to the column. Purified s-erbB proteins are buffer exchanged into 25 mM Hepes, 100 mM NaCl, pH 8.0, concentrated to between 20 and 100 μ M, and stored at 4° C. Purity was checked by SDS-PAGE, and concentrations were determined by absorbance at 280 nm using calculated extinction coefficients. Molar extinction coefficients used were s-erbB1, 58900; s-erbB2, 63310; s-erbB3, 68430; s-erbb4, 73550.

Multi-angle laser light-scattering (MALLS) studies

MALLS is our primary approach to study s-erbB homo- and heterodimerization. This technique is both more sensitive and more rapid than small-angle X-ray scattering that we have used before, allowing more experiments to be done, and over a wider range of protein concentrations. A DAWN DSP Laser Photometer from Wyatt Technologies (Santa Barbara, CA) is used, which is ideally suited to these experiments (Wyatt, 1993). The DAWN contains a glass flow-cell (volume 70 μ l), around which are 17 usable photodiode detectors at different angles from 15° to 160°. Scattering of light (633 nm) from a 5mW He-Ne laser is measured simultaneously at each of these angles, and normalized for variations in laser intensity as well as geometric effects (using an isotropic scatterer). The DAWN is used in micro-batch mode, samples being

Contains unpublished data

introduced into the flow-cell via a 0.1 μm filter with a syringe pump. To avoid introduction of air-bubbles, samples are degassed under vacuum, and introduced via a low dead-volume multi-port valve, which is loaded with several samples and purged of air prior to a series of measurements. A sample of 300 μl is more than sufficient to flush and equilibrate the flow-cell for stable scattering measurements, which themselves are observed in real time. With adjustments to the gain of the detector amplifiers, scattering from sEGFR samples of less than 0.01 mg/ml (0.1 μM) to greater than 10 mg/ml (100 μM) can be measured accurately. Data are collected and analyzed using the ASTRA software supplied with the instrument. For micro-batch experiments, we inject a series of samples with fixed sEGFR concentration and increasing concentrations of EGF. Scattering data at all 17 angles are collected until the response is stable. For a region of the normalized data after equilibration for each injected sample, the software is directed to calculate a Debye plot for each time point. In the Debye plot, $R(\theta)/K^*c$ is plotted against $\sin^2(\theta/2)$, where:

θ is the scattering angle

$R(\theta)$ is the excess intensity (I) of scattered light at that angle ($= I(\theta)_{\text{sample}}/I(\theta)_{\text{buffer}}$)

c is the mass concentration of the sample

K^* is a constant equal to $4\pi^2 n^2 (dn/dc)^2 / \lambda_0^4 N_A$, where n = solvent refractive index, dn/dc = refractive index increment of scattering sample, λ_0 = wavelength of scattered light, N_A = Avogadro's number

Since:

$$\frac{K^*c}{R(\theta)} = \frac{1}{\overline{M}_w P(\theta)} + 2A_2c \quad 1$$

where A_2 is the second virial coefficient, \overline{M}_w is the weight-averaged molecular mass, and:

$$P(\theta) = 1 - \frac{16\pi^2 R_G^2 \sin^2(\theta/2)}{3\lambda^2} + \dots \quad 2$$

then, extrapolating to zero angle $\theta = 0$ ($P(\theta) = 1$):

$$\frac{K^*c}{R(\theta)} = \frac{1}{\overline{M}_w} + 2A_2c \quad 3$$

By extrapolating the Debye plot to zero angle (when $R(\theta)/K^*c = \overline{M}_w$), the weight-averaged molecular mass (\overline{M}_w) of the molecule in the scattering sample can be measured directly if the value of the virial coefficient (A_2) is known for the protein. We have measured A_2 for s-erbB1 (and the 1:1 EGF:s-erbB1 complex) from Zimm plots, obtaining a value of $6.5 \times 10^{-5} \text{ mol.ml.g}^{-2}$. Even at the highest s-erbB1 concentrations studied (3mg/ml), A_2 contributes less than 3% to the apparent weight-averaged molecular mass. For monitoring s-erbB protein dimerization, we are interested

only in relative values of \overline{M}_w . If the concentration of receptor is fixed, errors in determination of the degree of glycosylation will not be important.

Analytical ultracentrifugation studies

Sedimentation equilibrium experiments employed the XL-A analytical ultracentrifuge (Beckman). Samples were loaded into six-channel epon charcoal-filled centerpieces, using quartz windows. Experiments were performed at 25°C using three different speeds (6,000 and 9,000, and 12,000 r.p.m.), detecting at 280 nm, with identical results. Solvent density was taken as 1.003 g/ml, and the partial specific volumes of the s-erbB proteins were approximated from their amino acid compositions and the assumption of approximately 20% carbohydrate, as 0.71 ml g⁻¹ for the purposes described in this report. Experiments were performed at 5 μM or 10 μM protein. Data were fit using the Optima XL-A data analysis software (Beckman/MicroCal) to models assuming a single ideal or non-ideal species for unliganded s-erbB proteins. When ligand was added, a two-species fit was used, in which one of the species was the excess ligand, which sediments as a 6 kDa (EGF) or 8 kDa (NRG) species. Knowing the K_D values from our BIAcore studies, the amount of free ligand is also known. The molecular mass of the s-erbB species is allowed to float in these fits. Fits were judged by the occurrence of randomly distributed residuals, examples of which are shown in Fig 6. Where possible, simple interpretation of analytical ultracentrifugation experiments was made by inspection.

BIAcore studies

Experiments employed a BIAcore 2000 instrument, and were all performed in 10 mM Hepes buffer, pH 7.4, containing 150 mM NaCl, 3.4 mM EDTA, and 0.005% Tween 20 at 25°C. Ligands were crosslinked to the hydrogel matrix of BIAcore CM5 Biosensor chips activated with *N*-hydroxysuccinimide (NHS) and *N*-ethyl-*N'*-[3-(diethylamino)propyl]carbodiimide (EDC). EGF at 200 μg/ml in 10 mM sodium acetate, pH 4.0 was then injected at 5 μl/min for 10 minutes. Non cross-linked EGF was removed, and unreacted sites were blocked with 1 M ethanolamine, pH 8.5. The signal contributed by immobilized EGF ranged from 150 RU to 400 RU, depending on the specific chip. For immobilization of NRG1-β1, the procedure was essentially the same, except that immobilization was performed in 10 mM sodium acetate at pH 4.8.

The purified s-erbB proteins at a series of concentrations were each flowed simultaneously over the EGF and NRG (and mock/control) surfaces at 5 μl/min for 7 minutes, by which time binding had reached a plateau in each case. The RU value corresponding to this plateau was taken as a measure of s-erbB protein binding, and was corrected for background non-specific binding and bulk refractive index effects by subtraction of data obtained in parallel using the mock-coupled

Contains unpublished data

hydrogel surface. RU values were then converted into percentage maximal binding. This conversion was performed separately for each surface (since levels of immobilization varied). 100% binding was defined for an NRG surface as the highest corrected signal seen with s-erbB3 and s-erbB4 (which were always the same to within 10%), and for an EGF surface the highest corrected signal seen with s-erbB1. Buffer washes between runs were sufficient to bring the RU value back down to baseline. Data were plotted as s-erbB concentration against percent maximal binding, and fit to a simple binding equation, in ORIGIN (MicroCal) to estimate K_D .

KEY RESEARCH ACCOMPLISHMENTS

- Produced and purified milligram quantities of the four erbB receptor extracellular domains for biophysical and structural studies
- Demonstrated that EGF induces homodimerization of the erbB1 (EGF receptor) extracellular domain, but of no other s-erbB protein
- Demonstrated that NRG induces homodimerization of the erbB4 extracellular domain, but of no other s-erbB protein
- Demonstrated that the erbB3 extracellular domain binds NRG1- β 1 without being induced to dimerize, and measured K_D values for ligand binding by other s-erbB proteins.
- Showed, for the first time, ligand-induced heterodimerization of isolated erbB receptor extracellular domains, with NRG1- β 1 inducing heterodimerization of s-erbB2 with either s-erbB3 or s-erbB4.
- Just as importantly, we have shown that s-erbB1 does not participate in any heterodimerization reactions, contrary to the expectations in the field.

REPORTABLE OUTCOMES

1. Results were presented at an invited lecture at the 1999 Gordon Conference on "Ligand Recognition and Molecular Gating" in Ventura, CA, March 7-12, 1999
2. Manuscript entitled: "Extracellular domains of erbB receptors are sufficient for ligand-induced homodimerization, but only neuregulin-induced heterodimerization", to be submitted to *EMBO Journal*, September 1999.

CONCLUSIONS

Our studies to date alter the view of erbB receptor activation by EGF and NRG family members. ErbB1 and erbB4 are the central receptors in the system, binding to and being homodimerized by EGF and NRG respectively. Transmodulation of erbB2 by NRG, to which it does not bind directly, appears to involve NRG-induced formation of heterodimers with erbB3 or erbB4. These heterodimers can be recapitulated using isolated extracellular domains. So far, these findings - observed *in vitro* for the first time - are consistent with expectations from previous cellular studies. A major contribution here is to show that the s-erbB2/s-erbB4 heterodimer, for example, is indeed a hetero**D**imer, and not a larger aggregate. This question has not been addressed before. A major surprise in our studies was the inability of s-erbB1 to form heterodimers, in spite of the fact that interactions (of unknown stoichiometry) between erbB1 and erbB2 sparked much of the debate about erbB receptor heterodimerization.

Our findings argue:

1. That erbB1 (EGFR) activation is mechanistically distinct from EGF-induced transmodulation of erbB2, erbB3, and erbB4. We hypothesize that oligomers involving erbB1 homodimers must be formed, and we are performing experiments to test this.
2. That EGF and NRG activate erbB2 through distinct mechanisms: one (NRG) through ligand-induced heterodimer formation, and the other (EGF) through an as-yet-unclear mechanism. Experiments, described in Tasks 2 and 3 of the approved Statement of Work will now be performed to distinguish between these possibilities.
3. While our supposition going into this project was that quantitative differences would explain the diversity of signaling in this system, the studies to date have identified qualitative differences that are more likely to be of use in design of therapeutic strategies.

So What ?

A major aim in breast cancer is to inactivate or otherwise remove erbB2/Neu/Her2 in the 30% or so of cases where its over-expression is seen. Herceptin has this as the basis of its efficacy. Our studies are bringing new insights into how erbB2 is regulated in cells. In particular we find that there are TWO mechanisms for erbB2 transmodulation by other receptors in the erbB family. Since breast cancer cells differ in their complement of other erbB receptors, these mechanisms are likely to be of different degrees of importance in different cases (T47D cells and SKBR-3 cells will differ, for example). Understanding the mechanisms, which we are beginning to do, will allow us to begin our approaches to designing new strategies for intervention when erbB2 is inappropriately active. Knowing when the different mechanisms are most important will allow consideration of approaches that are much more selective and specific than can possibly be true with antibody-based therapies.

REFERENCES

- Ballinger, M.D., Jones, J.T., Lofgren, J.A., Fairbrother, W.J., Akita, R.W., Sliwowski, M.X., and Wells, J.A. (1998) Selection of heregulin variants having higher affinity for the ErbB3 receptor by monovalent phage display. *J. Biol. Chem.* **273**, 11675-11684.
- Brown, P.M., Debanne, M.T., Grothe, S., Bergsma, D., Caron, M., Kay, C., and O'Connor-McCourt, M.D. (1994) The extracellular domain of the epidermal growth factor receptor. Studies on the affinity and stoichiometry of binding, receptor dimerization and a binding-domain mutant. *Eur. J. Biochem.*, **225**, 223-233.
- Cohen, B.D., Green, J.M., Foy, L., Fell, H.P. (1996) HER4-mediated biological and biochemical properties in NIH 3T3 cells. Evidence for HER1-HER4 heterodimers. *J. Biol. Chem.* **271**, 4813-4818.
- Fitzpatrick, V.D., Pisacane, P.I., Vandlen, R.L., and Sliwkowski, M.X. (1998) Formation of a high-affinity heregulin binding site using the soluble extracellular domains of ErbB2 with ErbB3 or ErbB4. *FEBS Letts.* **431**, 102-106.
- Greenfield, C., Hiles, I., Waterfield, M.D., Federwisch, M., Wollmer, A., Blundell, T.L., and McDonald, N. (1989) Epidermal growth factor binding induces a conformational change in the external domain of its receptor. *EMBO J.*, **8**, 4115-4123.
- Günther, N., Betzel, C., and Weber, W. (1990) The secreted form of the epidermal growth factor receptor: Characterization and crystallization of the receptor-ligand complex. *J. Biol. Chem.*, **265**, 22082-22085.
- Holmes, W.E., Sliwkowski, M.X., Akita, R.W., Henzel, W.J., Lee, J., Park, J.W., Yansura, D., Abadi, N., Raab, H., Lewis, G.D., Shepard, H.M., Kuang, W.-J., Wood, W.I., Goeddel, D.V., and Vandlen, R.L. (1992) Identification of heregulin, a specific activator of p185^{erbB2}. *Science* **256**, 1205-1210.
- Horan, T., Wen, J., Arakawa, T., Liu, N., Brankow, D., Hu, S., Ratzkin, B., and Philo, J.S. (1995) Binding of Neu differentiation factor with the extracellular domain of Her2 and Her3. *J. Biol. Chem.* **270**, 24604-24608.
- Hurwitz, D.R., Emanuel, S.L., Nathan, M.H., Sarver, N., Ullrich, A., Felder, S., Lax, I., and Schlessinger, J. (1991) EGF induces increased ligand binding affinity and dimerization of soluble epidermal growth factor (EGF) receptor extracellular domain. *J. Biol. Chem.*, **266**, 22035-22043.
- Jones, J.T., Ballinger, M.D., Pisacane, P.I., Lofgren, J.A., Fitzpatrick, V.D., Fairbrother, W.J., Wells, J.A., and Sliwowski, M.X. (1998) Binding interaction of the heregulin β egf domain with erbB3 and erbB4 receptors assessed by alanine scanning mutagenesis. *J. Biol. Chem.* **273**, 11667-11674.
- Jones, J.T., Akita, R.w., and Sliwkowski, M.X. (1999) Binding specificities of egf domains for ErbB receptors. *FEBS Letts.* **447**, 227-231.
- Kashles, O., Yarden, Y., Fischer, R., Ullrich, A., and Schlessinger, J. (1991) A dominant negative mutation suppresses the function of normal epidermal growth factor receptors by heterodimerization. *Mol. Cell. Biol.* **11**, 1454-1463.

- King, C.R., Borrello, I., Bellot, F., Comoglio, P., and Schlessinger, J. (1988) EGF binding to its receptor triggers a rapid tyrosine phosphorylation of the erbB2 protein in the mammary tumor cell line SKBR-3. *EMBO J.* **7**, 1647-1651.
- Lax, I., Mitra, A.K., Ravera, C., Hurwitz, D.R., Rubinstein, M., Ullrich, A., Stroud, R.M., and Schlessinger, J. (1991a) Epidermal growth factor (EGF) induces oligomerization of soluble, extracellular, ligand-binding domain of EGF receptor. *J. Biol. Chem.*, **266**, 13828-13833.
- Lemmon, M.A., Bu, Z., Ladbury, J.E., Zhou, M., Pinchasi, D., Lax, I., Engelman, D.M., and Schlessinger, J. (1997) Two EGF molecules contribute additively to stabilization of the EGFR dimer. *EMBO J.* **16**, 281-294.
- Qian, X., Dougall, W.C., Hellman, M.E., and Greene, M.I. (1994) Kinase-deficient *neu* proteins suppress epidermal growth factor receptor function and abolish cell transformation. *Oncogene* **9**, 1507-1514.
- Spivak-Kroizman, T., Rotin, D., Pinchasi, D., Ullrich, A., Schlessinger, J., and Lax, I. (1992) Heterodimerization of c-erbB2 with different epidermal growth factor receptor mutants elicits stimulatory or inhibitory responses. *J. Biol. Chem.* **267**, 8056-8063.
- Stern, D.F., and Kamps, M.P. (1988) EGF-stimulated tyrosine phosphorylation of p185^{neu}: A potential model for receptor interactions. *EMBO J.* **7**, 995-1001.
- Tzahar, E., Pinkas-Kramarski, R., Moyer, J.D., Klapper, L.N., Alroy, I., Levkowitz, G., Shelly, M., Henis, S., Eisenstein, M., Ratzkin, B.J., Sela, M., Andrews, G.C., and Yarden, Y. (1997) Bivalence of EGF-like ligands drives the ErbB signaling network. *EMBO J.* **16**, 4938-4950.
- Wada, T., Qian, X., and Greene, M.I. (1990) Intermolecular association of the p185^{neu} protein and EGF modulates EGF receptor function. *Cell* **61**, 1339-1347.
- Wyatt, P.J. (1993) Light scattering and the absolute characterization of macromolecules. *Analytica Chimica Acta* **272**, 1-40.
- Zhang, K., Sun, J., Liu, N., Wen, D., Chang, D., Thomason, A., and Yoshinaga, S.K., (1996) Transformation of NIH3T3 cells by HER3 or HER4 receptors requires the presence of HER1 or HER2. *J. Biol. Chem.* **271**, 3884-3890.
- Zhou, M., Felder, S., Rubinstein, M., Hurwitz, D.R., Ullrich, A., Lax, I., and Schlessinger, J. (1993) Real-time measurements of kinetics of EGF binding to soluble EGF receptor monomers and dimers support the dimerization model for receptor activation. *Biochemistry*, **32**, 8193-8198.



DEPARTMENT OF THE ARMY
US ARMY MEDICAL RESEARCH AND MATERIEL COMMAND
504 SCOTT STREET
FORT DETRICK, MARYLAND 21702-5012

REPLY TO
ATTENTION OF:

MCMR-RMI-S (70-1y)

28 May 02

MEMORANDUM FOR Administrator, Defense Technical Information Center (DTIC-OCA), 8725 John J. Kingman Road, Fort Belvoir, VA 22060-6218

SUBJECT: Request Change in Distribution Statement

1. The U.S. Army Medical Research and Materiel Command has reexamined the need for the limitation assigned to technical reports written for Grant DAMD17-98-1-8232. Request the limited distribution statements for Accession Documents Number ADB258643 and ADB266202 be changed to "Approved for public release; distribution unlimited." These reports should be released to the National Technical Information Service.

2. Point of contact for this request is Ms. Judy Pawlus at DSN 343-7322 or by e-mail at judy.pawlus@det.amedd.army.mil.

FOR THE COMMANDER:

A handwritten signature in cursive script, appearing to read "Phyllis M. Rinehart", is positioned above the typed name and title.

PHYLLIS M. RINEHART
Deputy Chief of Staff for
Information Management